Activated olive mill waste-based hydrochars as selective adsorbents for CO_2 capture under postcombustion conditions

Belén González*, Joan J. Manyà

Aragón Institute of Engineering Research (I3A), Technological College of Huesca, University of Zaragoza, crta. Cuarte s/n, Huesca E-22071, Spain

* Corresponding author at: Technological College of Huesca, University of Zaragoza, Crta. Cuarte s/n, Huesca E-22071, Spain.

E-mail address: belenglez@unizar.es (Belén González).

Keywords

Olive mill waste; Hydrothermal carbonization; Activation; Postcombustion CO_2 capture; Nitrogen doping.

ABSTRACT

Porous carbons are considered to be promising sorbents for carbon capture and sequestration. As precursors, the use of biomass materials has acquiring special interest due to its low cost and high availability. Among all the possibilities to convert low-value biomass into these interesting sorbents, hydrothermal carbonization has demonstrated several advantages such as lower energy consumption over pyrolysis. In this work, activated hydrochars using two-phase olive mill waste as precursor have been prepared through physical and chemical activation using CO_2 and KOH, respectively. Additionally, with the aim to study the influence of the nitrogen on their adsorption capacity, N-doped adsorbents have been prepared through a one-step hydrothermal carbonization. The behaviour of these adsorbents has been studied in terms of CO_2 uptake capacity at an absolute pressure of 15 kPa and temperatures of 0, 25 and 75 ºC, apparent selectivity towards CO_2 over N_2, and isosteric heat of adsorption. Among all these samples, the physically activated hydrochar appears to be the best due to its higher CO_2 uptakes, adsorption rates and values of selectivity at 25 ºC. Therefore, considering these results, doping these materials with nitrogen does not appear to enhance their adsorption properties, contrary to what some authors have previously reported.

1. Introduction

Although the growth of non-fossil fuel consumption is a reality, it seems that the dependence on fossil fuels for energy supply will be still very strong in the closest future. Therefore, there is still an urgent necessity to reduce the CO_2 emissions. Among all the technologies studied, CO_2 capture and geological storage is considered to be a major mitigation option for climate change. Of the different approaches available for capturing CO_2, adsorption with solids has been pointed to be one of the most promising strategies due to the low cost of their synthesis and the low energy penalties these technologies present when comparing with other processes [1].

Among all the solids adsorbents studied until now, carbonaceous adsorbents have shown several advantages towards other tested materials as zeolites, calcium oxides, hydrotalcites or metal-organic frameworks (MOFs) among others. Their higher resistance to moisture, higher thermal, mechanical and chemical stability and low energy requirements and price, make of these materials the most attractive adsorbents to capture CO_2 [1].

Moreover, when waste biomass is used as precursor of these sorbents, its attractiveness for the CO_2 capture process increases because of the relative ease and low cost of their synthesis [2]. Several have been the processes studied during the last years to convert this waste biomass on valuable carbon materials. Among all the possibilities to convert low-value biomass into these interesting sorbents, HTC (hydrothermal carbonization) has demonstrated several advantages such as lower energy consumption over pyrolysis. Feedstocks with a high moisture content yield low amounts of solid material after drying, which makes them insufficient sources for pyrolysis. Therefore, a greater variety of feedstocks could be considered for processing into hydrochar since drying the feedstock is not necessary for HTC. Another advantage is that HTC yields higher amounts of char and uses lower amounts of energy than pyrolysis [3].

As several authors have previously reported, the physical properties of the sorbent depend mainly on the nature of the precursor. A wide number of biomass precursors have been studied until the date: rice husks [4], vine shoots [5], almond shells [6], coconut shells [7], among others. In all the cases, the raw material is converted into biochar or hydrochar (through pyrolysis and hydrothermal carbonization, respectively) and therefore, activated either physically or chemically with the aim to get the higher quantity of ultra-micropores (pore size < 0.7 nm) in their structure. Previous authors [4, 8] agreed that as highest was the amount of ultra-micropores in the studied activated carbons, highest was their CO_2 adsorption capacity. These works concluded that the high selectivity CO_2/N_2 and the excellent cyclability that these materials showed were more related to the big amount of ultra-micropores presented in their structures than with their specific surface area. This theory was more recently confirmed by Manyà et al. [5] who found that among all the sorbents studied in their work, the highest ultra-micropore volume was obtained for the activated carbon with a highest KOH/biochar ratio, which showed at the same time the major CO_2 uptake capacity at the experimental conditions studied (0 ºC and 15 kPa).

In this attempt to find the adsorbents with the best capacities, a controversy regarding the role of the nitrogen-functional groups when incorporating to the porous carbons has come on. While some authors [9–11] advocate for the positive effect that N-doping has on the materials, improving their CO_2 capture capacity and heats of adsorption, others [12–14] have demonstrated that the presence of nitrogen in the porous structure does not influence on their CO_2 uptake.

Among these last, Adeniran et al. [13] demonstrated that after comparing some carbons doped with N with other undoped, all of them prepared with similar pore size distribution, no any beneficial regarding the CO_2 uptake was observed. Similar conclusions had been previously obtained by Sevilla et al. [12] and Kumar et al. [14]. While Sevilla et al. [12] found

that the presence of N did not have any appreciable effect on CO_2 adsorption, the second [14] appreciated a marginal improvement of the N-doped adsorbents comparing with the undoped ones being the real effect observed on the CO_2/N_2 selectivity, which increased in the case of the nitrogen-enriched materials. Both works agree that the CO_2 uptake of these carbons depends, independently of the presence of N, on the pore distribution and more in particular on the proportion of ultra-micropores present in their structures.

However, on the other hand, there are some authors [9–11] who reported that the incorporation of nitrogen-functional groups into the carbon structure enhances the interaction with CO_2 of these materials. Among others works, Xu et al. [15] measured capacities up to 5.86 mmol g^{-1} at 101.3 kPa and 0 °C for a nitrogen-doped carbon prepared from tree leaves and activated at 600 ºC. Similar values were achieved by Yue et al. [9] who synthetized porous nitrogen-doped carbons by carbonization of coconut shell followed by urea modification and K_2CO_3 activation. In this last case, the adsorbents showed CO_2 uptakes of 3.71 mmol g^{-1} at 101.3 kPa and 25 ºC and 5.12 mmol g^{-1} at 0 ºC.

Therefore, one of the objectives of this work is to elucidate both, the effect of N-doping as well as the effect of the pore size distribution on the CO_2 capture capacity of these porous adsorbents.

The growth that the industry of oil production has suffered in the last decades, not only in the Mediterranean countries but also in other countries as Serbia and Montenegro, Macedonia, Cyprus, Turkey, Israel, Jordan, the USA, Australia, the Middle East and specially in China [17] has exacerbated the environmental problems due to the production of high amounts of by-products: olive pomace (OP) and olive mill wastewater (OMW) [18]. In Spain, the introduction of the two-phase centrifugation system for oil extraction during the decade of 90´s reduced the production of wastewater generation, still produced approximately four million tons per year of a solid olive-mill by-product called “alperujo” or two-phase olive mill

waste (TPOMW). Characterization experiments of these samples have shown that this product has a high moisture content, slightly acidic pH values and a very high content of organic matter (lignin, hemicellulose and cellulose) [19]. Although several attempts to reuse the TPOMW disposal have been made as its use for the co-generation of electrical power, the necessity to find less expensive uses has led to research into new ways. One possibility is to use it for the preparation of soil organics fertilizers and amendments; however, its direct application to the soil has been demonstrated to effect negatively the soil structural stability, seed germination, plant growth and microbial activity [19]. Another potential application which is being under study is its use to develop sorbents for CO_2 capture. As it was introduced above, the use of biomass as a precursor of these sorbents presents several advantages and in this work, activated carbons using TPOMW as precursor have been prepared. Considering the already summarized advantages that hydrochar presents when comparing with biochar, hydrochars from this biomass were produced and then, activated following different processes. The final objective is to study the CO_2 capture capacity of these sorbents under postcombustion conditions. Both, physical activation with CO_2 and chemical activation with KOH processes were used to study their effect on the properties of the prepared hydrochars and its behaviour as CO_2 adsorbents. Besides, N-doped adsorbents have been prepared through a one-step hydrothermal carbonization to study the effect of nitrogen-doping in terms of CO_2 uptake. These doped carbons were also physically activated with the same method used with the other hydrochars.

In this work, the CO_2 adsorption capacities of the developed sorbents were measured at 0, 25 and 75 ºC and at CO_2 pressure of 15 kPa (the normal value in postcombustion conditions). On the other side, the CO_2/N_2 selectivities were measured at 25 ºC and 101.3 kPa in a thermogravimetric analyser under pure CO_2 or N_2 environment.

2. Materials and methods

2.1.Materials

The material used in this study was prepared by hydrothermal carbonization of the two-phase olive mill waste supplied by the company Ecostean, an olive oil manufacturer from Huesca (Spain). Results from proximate and elemental analyses as well as ash composition for the olive mill waste are given in the Supplementary Data. The pyrolysis device and the experimental procedure have been described in detail elsewhere [20, 21]. The HTC experiments were carried out in a 100 mL Parr reactor (reactor series 4590) able to work up to a pressure of 35 MPa and a temperature of 350 ºC. The reaction temperature was controlled using a Parr proportional-integral-derivative (PID) controller (Model 4858).

2.2. Activation

The hydrochar materials produced were activated by both physical and chemical methods. For physical activation, 10 g of hydrochar was heated at 10 °C min^{-1} to 700 or 850 °C under a steady flow of CO_2 (100 mL min^{-1} STP) in a vertical fixed-bed quartz reactor (25 mm ID) at atmospheric pressure. Physically hydrochars were obtained at two different holding times at these temperatures (1 and 3 h) and denoted as *AC_HTC_CO2_Y_X*, where *Y* corresponds to the activation temperature and *X* corresponds to the holding time in hours.

For chemical activation with KOH, 10 g of hydrochar was physically mixed with KOH (particle size lower than 1.5 mm) in a mortar at two KOH/hydrochar mass ratios (2/1 and 5/1). The resulting mixtures were then heated under N_2 (100 mL min^{-1} STP) to 600 or 700 °C (holding time at the final temperature = 30 min) in the same fixed-bed quartz reactor mentioned above at an average heating rate of 10 °C min^{-1}. Chemically hydrochars are denoted as *AC_HTC_KOH_X_Y*, where *X* is the mass of KOH per mass unit of hydrochar and *Y* corresponds to the final temperature reached during heating in °C.

For the synthesis of N-doped carbon materials, two-phase olive mill waste, $ZnCL_2$, Pyrrole-2-carboxaldehyde at three mass percentages (37.5, 56.25 and 6.25 %) and 1.5 ml of H_2O were thoroughly mixed. The mixture was then transferred to a glass vessel that was introduced in a Teflon-lined autoclave and kept at 200 °C under autogenous pressure for 24 hours. After hydrothermal synthesis, the solid was directly dried at 110 °C in an oven, without any previous washing. Finally, a physical activation following the procedure described above was carried out, where the hydrochar was heated at 10 °C min^{-1} to 700 °C under a steady flow of CO_2 or N_2. These one-pot hydrochars are denoted as *AC_HTC_ZN_X_Y_Z*, where *X* is the temperature reached during heating, *Y* is the gas used for the activation and *Z* corresponds to the holding time. Fig 1. summarizes the different production pathways described above for the different materials studied in this work.

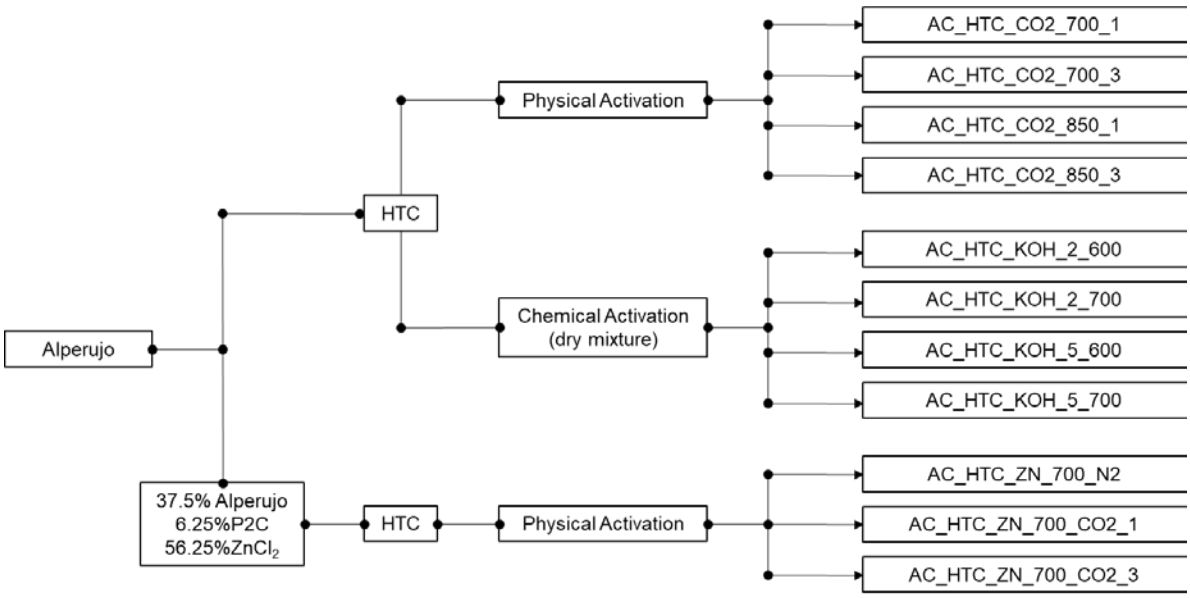

Fig 1. Graphical scheme of the production pathways for all the two phase olive mill waste-derived absorbents studied in this work.

2.3.Characterization

N_2 adsorption/desorption isotherms at –196 °C were obtained using an ASAP 2020 gas sorption analyzer from Micromeritics (Norcross, GA, USA). Samples were previously degassed under dynamic vacuum conditions to constant weight at a temperature of 150 °C. Apparent specific surface areas (S_{BET}) were calculated using the Brunauer–Emmet–Teller (BET) model at small relative pressures (p/p_0 = 0.01–0.15). Total pore volume (V_t) was determined from the specific volume of N_2 adsorbed at a relative pressure of 0.99. The t-plot method (carbon black STSA thickness equation) was used to estimate the micropore volume (V_{mic}, for pore sizes lower than 2 nm). Ultra-micropore size distributions and the ultra-micropore volume (V_{ultra}, for pore sizes lower than 0.7 nm) of carbons were estimated from their CO_2 adsorption isotherms at 0 °C, which were measured using the same analyzer described above under the same degassing conditions. For this purpose, a Density Functional Theory (DFT) method assuming slit-pore geometry was employed. Given that some adsorbents could contain mainly ultra-micropores (especially the non-activated biochars), S_{BET} values were also estimated for a proper linear region from the CO_2 adsorption data at 0 °C. Recently, Kim et al. [22] have reported that the BET specific surface areas from CO_2 at 0 °C can be considered as reasonable proxies for highly ultra-microporous materials. Finally, the micropore volumes (V_{DA}) assuming the Dubinin-Astakhov model were estimated from the CO_2 adsorption data. All the necessary calculations from both N_2 and CO_2 adsorption isotherms were performed using the MicroActive software (v. 4.03) supplied by Micromeritics Instrument Corp.

2.4. CO_2 uptake and selectivity

The CO_2 adsorption capacities at 25 and 75 °C were measured using the ASAP 2020 gas sorption analyzer. Samples (around 120–200 mg) were degassed under the same conditions above-mentioned.

To estimate the apparent selectivity towards CO_2 over N_2, adsorption experiments at atmospheric pressure (under pure CO_2 or N_2) were conducted in a thermogravimetric analyzer (TGA) composed of a MK2 microbalance (precision of 0.1 μg) from CI Precision (UK). Samples (with an initial mass of around 15 mg) were firstly degassed under a steady flow of He (100 mL min^{-1} STP) at 150 °C for 1 h. After cooling to 25°C, carrier gas was switched from He to CO_2 or N_2 (100 mL min^{-1} STP).

3. Results and discussion

3.1.Porous properties and CO_2 adsorption capacity at 0℃

Isotherms of adsorption of N_2 at –196 °C and CO_2 at 0 °C (see Fig. 2) were used to determine specific surface area, pore volume and textural characteristics of the pores. All the data are summarized in Table 1. From these results, it is observed that for the physically activated samples, as higher are the temperature and time of activation, bigger are the values of S_{BET} determined from the N_2 adsorption isotherms. Hence, that the highest value of S_{BET} is obtained for the AC_HTC_CO2_850_3 sample (1135 m^2 g^{-1}), which is much higher than the determined by previous authors for physically activated samples although within the common range reported in the literature for biomass-derived activated carbons [5, 6, 8, 23–25]. Regarding the chemically activated samples, the AC_HTC_KOH_5_700 sample is the one which shows the biggest S_{BET}, obtaining, also in this case, higher values of S_{BET} as the temperature of activation increased. Contrary to what happened with the physically activated samples, all the chemically activated carbons, excluding the AC_HTC_KOH_2_600 which

presents the lowest value of S_{BET} among all the samples studied in this work (3.7 m^2 g^{-1}), show values of S_{BET} within the common range reported for chemically activated carbons with KOH [5, 23–25]. This last sample, as it happens with the physically activated AC_HTC_CO2_700_1 (S_{BET} of 26.1 m^2g^{-1}), presents very low values of S_{BET} because both samples possess mostly ultra-micropores and at cryogenic temperatures, the diffusion rate of the N_2 molecules into this size of micropores is very low [22]. Therefore, it is not possible to determine the total pore volume (V_t) and the micropore volume (V_{mic}) for both carbons using the t-plot method and this is the reason why these values for these materials are showed as NA in Table 1. Finally, for the one-pot synthetized samples, it could be observed that the three of them present values of S_{BET} very similar to the values reported by previous authors for N-doped carbons [11, 13, 16, 26] being the one activated in a N_2 atmosphere which presents the highest value (937 m^2 g^{-1}). Besides, as it was previously found by other authors [11, 16], these last samples present a higher percentage of mesopores when comparing with the rest of materials. According to these researchers, the presence of nitrogen inhibits the formation of micropores in favour of mesopores and this would explain the lower CO_2 uptakes showed by the N-enriched carbons.

Table 1. Textural properties and CO_2 uptake (at 0°C) of the two-phase olive mill waste derived carbons.

Sample	Apparent specific surface area (m^2g^{-1})			Specific pore volume ($cm^3\ g^{-1}$)				CO_2 uptake at 0ºC (mmol g^{-1})	
	S_{BET} [a]	S_{BET} [b]	S_L [b]	V_t	V_{mic}	V_{meso}	V_{ultra}	15 kPa	101.3 kPa
AC_HTC_CO2_700_1	26.1	220	176	NA	NA	NA	0.096	1.050	1.409
AC_HTC_CO2_700_3	97.1	224	158	0.027	0.0253	NA	0.078	0.904	1.260
AC_HTC_CO2_850_1	576	372	386	0.228	0.1878	0.002	0.134	1.375	2.595
AC_HTC_CO2_850_3	1135	424	435	0.476	0.373	0.014	0.153	1.542	2.945
AC_HTC_KOH_2_600	3.7	189	173	NA	NA	NA	0.068	0.758	1.262
AC_HTC_KOH_2_700	888	460	482	0.392	0.294	0.027	0.159	1.350	2.984
AC_HTC_KOH_5_600	627	361	311	0.277	0.1985	0.020	0.136	1.487	2.342
AC_HTC_KOH_5_700	1036	555	588	0.449	0.3455	0.024	0.192	1.550	3.521
AC_HTC_ZN_700_CO2_1	883	485	520	0.513	0.243	0.204	0.198	1.089	2.759
AC_HTC_ZN_700_CO2_3	760	371	422	0.405	0.216	0.133	0.133	0.856	2.210
AC_HTC_ZN_700_N2	937	375	404	0.518	0.263	0.185	0.127	0.978	2.290

[a] calculated from N_2 adsorption data a –196°C.

[b] calculated from CO_2 adsorption data a 0°C.

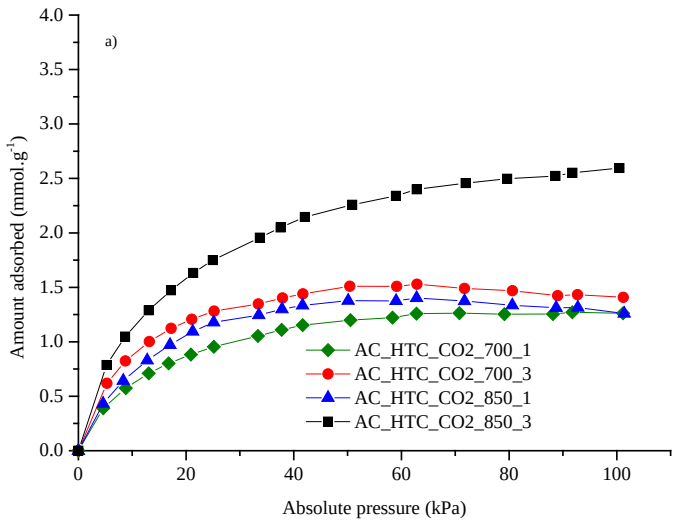

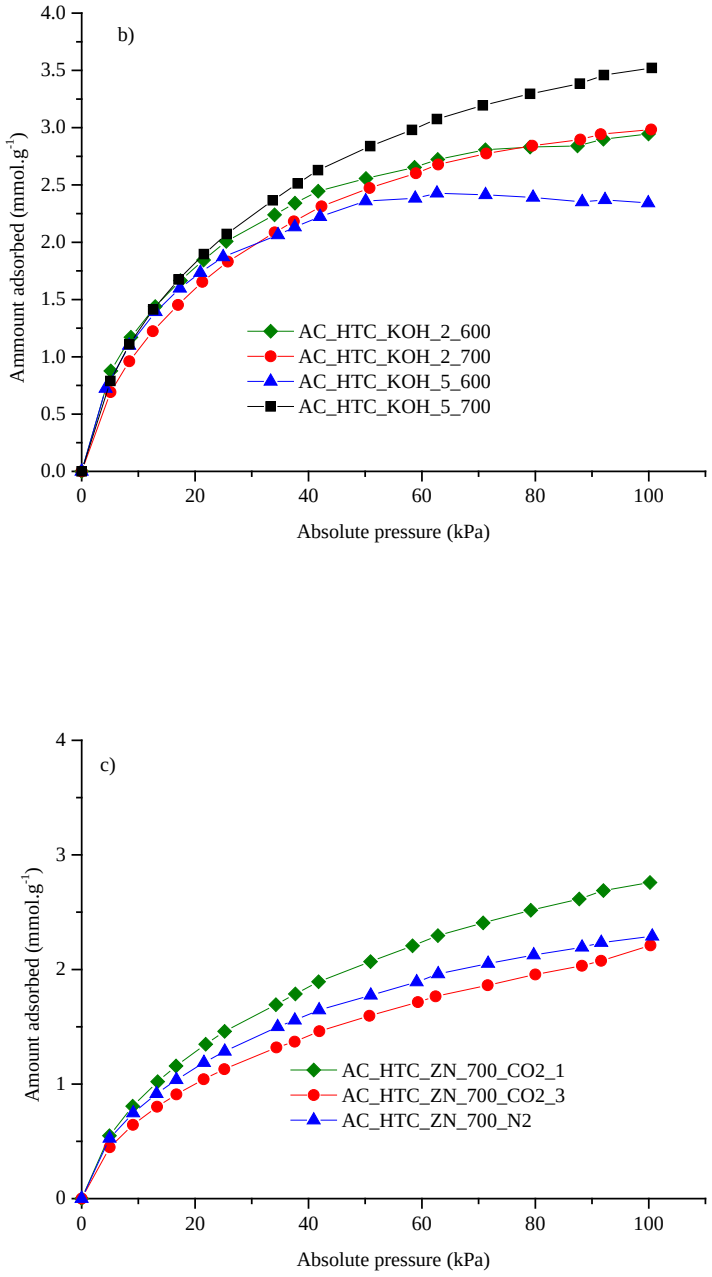

Fig 2. CO_2 adsorption isotherms (at 0ºC) for (a) HTCs physically activated, (b) HTCs chemically activated with KOH using the dry mixture method and (c) one-pot synthetized samples.

Table 1 also reports the Langmuir surface areas (S_L), which were also determined from the CO_2 adsorption isotherms at 0 °C. In this sense, a reasonable agreement between both models was found by Manyà et al. [5] given that the range of relative pressures selected for the estimation of both the S_{BET} and S_L values was the same (0.01–0.02). However, contrary to what

Manyá et al.[5] observed for the materials they studied, no any linear correlation between S_{BET} and V_{ultra} was found for any of the groups of hydrochars investigated in this work.

The values of the ultra-micropore volume estimated using a DFT-based model for all the samples studied in this work are also summarized in Table 1. As it can be seen, this value is especially high for the AC_HTC_KOH_5_700 (0,192 cm^3 g^{-1}) and AC_HTC _ZN_700_CO2_1 (0,198 cm^3 g^{-1}) samples. Some previous works [2, 4, 5, 8, 27] reported high values of ultra-micropore volume (also estimated using DFT or NLDFT methods) for the ACs studied (up to 0.148 cm^3g^{-1}) but it was not until recently that Xu et al.[11] and Liu et al. [27] found values so elevated as the showed by these two hydrochars investigated in this work. Xu et al. [11] obtained, using a DFT-based model, values of V_{ultra} between 0.171 and 0.209 cm^3g^{-1} for camphor leaves chemically activated with KOH at different temperatures. All the activated carbons studied by Xu et al. [11] showed a very strong peak at 0.6 nm, which would explain the higher CO_2 uptake showed by these materials comparing with the works previously mentioned and the hydrochars studied here. On the other hand, Liu et al. [27] studied dried rice husk samples pre-oxidized and impregnated with KOH, which were compacted at different pressures. From the results obtained, the authors highlighted the V_{ultra} value obtained for the R7_2T_10PEI carbon sample, which had the highest ultra-microporosity (0.175 cm^3/g) with a mono-modal pore size distribution centred at 0.37 nm (a value a bit higher than the dynamic diameter of CO_2 molecules, 0.34 nm). Nevertheless, in spite of possessing similar values of V_{ultra} than the reported by Liu et al. [27] and Xu et al. [11], the two samples studied here do not present CO_2 uptakes so high as the values reported by these two authors in their works. This could be explained, as it was mentioned above, because of the high percentage of mesoporous presented by these materials. The ultra-micropore size distributions determined from the CO_2 adsorption using the DFT-based model are shown in Fig. 3 for the samples investigated in this work. Comparing the values obtained for all the samples studied, it could be observed that the

sample with the highest ultra-micropores volume is the one synthesized using one-step hydrothermal process AC_HTC_ZN_700_CO2_1. However, this value does not correspond to the highest CO_2 adsorption capacity at 0 °C and 15 kPa (see Table 1) as it would be expected, according to previous authors [5, 8], who found a proportional relation between both parameters. In this sense, as it was stated in the introduction section, there is a controversy regarding the effect of nitrogen-doping on the CO_2 capture capacity of these materials. While several authors reported a negligible effect of nitrogen over the CO_2 capture capacity of the carbons [12–14], others [9–11] found a positive effect on the CO_2 uptakes and heat of adsorption of the materials.

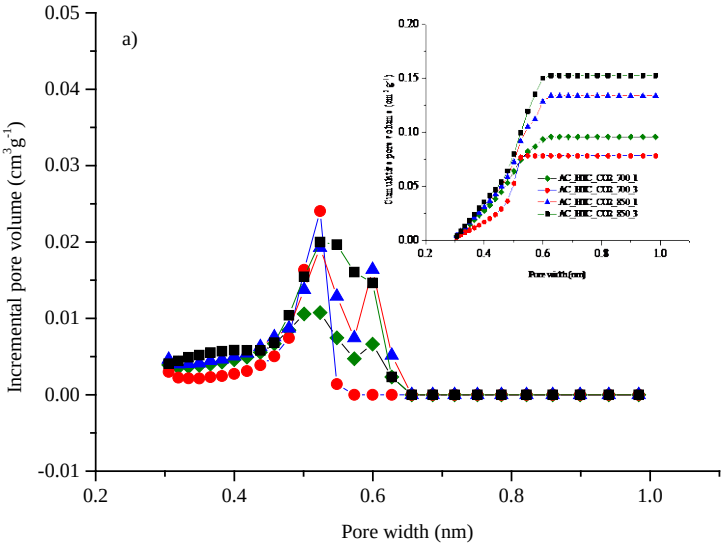

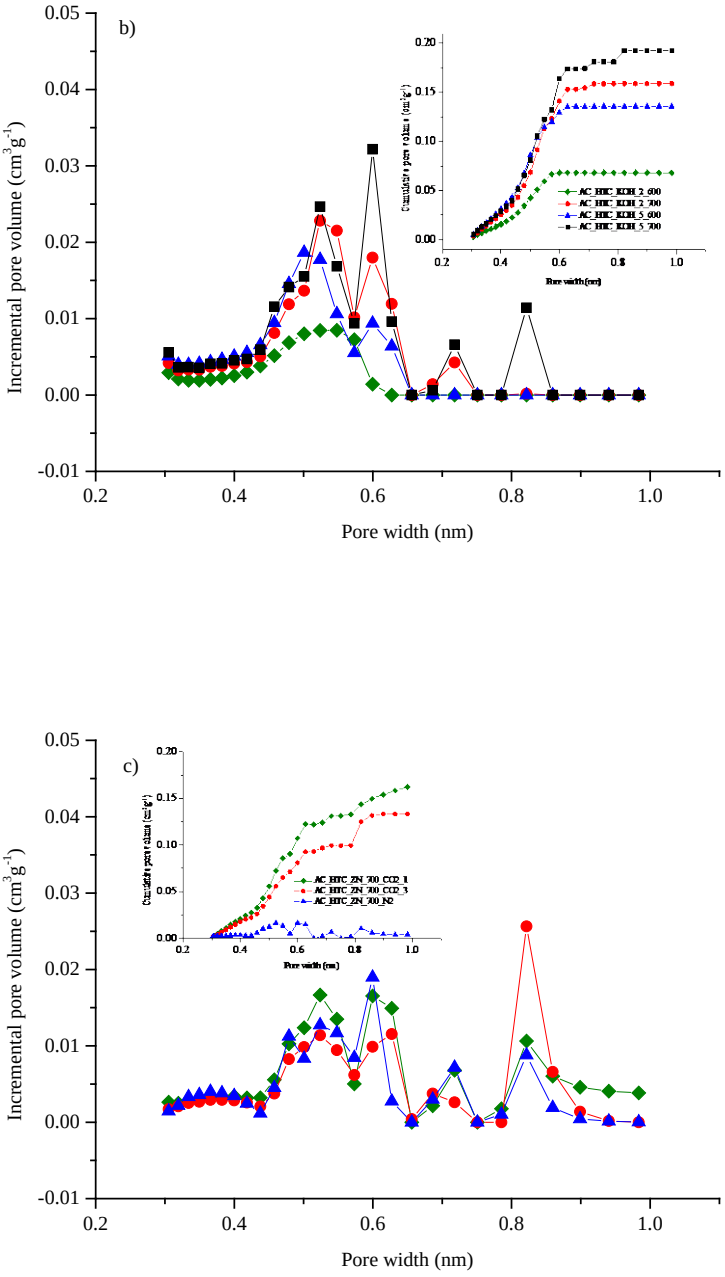

Fig 3. Utra-micropore size distributions for (a) HTCs physically activated (b) HTCs chemically activated with KOH using the dry mixture method and (c) one-pot synthetized samples.

Considering the values summarized in Table 1, we can see in the three cases, that when comparing the N-doped carbons with the undoped ones with similar V_{ultra}, the CO_2 capture capacity is slightly lower for the N-enriched materials. Therefore, these results agree with the

conclusions reported by the first authors mentioned above [12–14] and are in contrast to the works [10, 15, 26] which claim on the benefits of nitrogen functionalities on carbon. Based on this lack of agreement, further investigations would be necessary to elucidate the role of nitrogen-doping on CO_2 adsorption of these porous carbons. In this sense, according to Kumar et al. [14], studying the effect of N over the CO_2 uptake only through experimental work is very difficult due to the variety of parameters involved and that have not been considered in the works published up to date. Two of these factors are the presence of additional functional groups and the pore architecture, among others.

On the other hand, still from the results shown in Table 1, it can be observed that are the chemically activated samples which present the highest CO_2 adsorption capacities. In particular, it is the sample AC_HTC_KOH_5_700 which presents the highest uptake (0.155 mmol g^{-1} at 15 kPa and 0 ºC) among all the samples studied. When comparing the value showed by the AC_HTC_KOH_5_700 sample with the obtained for the other chemically activated samples using the same method but different rates and temperatures, it is observed that the results obtained confirm the conclusion reported by Manyá et al. [5], who said that higher KOH/biochar ratios can promote the formation of pores with sizes above 0.7 nm. Moreover, according with this previous work [5], samples activated with a ratio of 5 show higher values of V_{mic} than the same samples activated with a ratio of 2 at similar temperature.

Regarding the undoped samples, it is observed that the CO_2 capture capacities (at 0 °C and 15 kPa) of all the hydrochars studied in this work are quite similar and agree with the values obtained by previous studies for similar materials [4, 6–8, 24, 25, 28–30]. Among all the values shown in Table 1, it must be highlighted the values obtained for the physically hydrochar activated at 850 °C during 3 h (1.54 mmol g^{-1}) and the one obtained for the already mentioned AC_HTC_KOH_5_700 sample (1.55 mmol g^{-1}). A bit lower are the values obtained for the chemically activated sample at similar temperature but with a ratio of 2 (1.35 mmol g^{-}

^{1}) and with a similar ratio but activated at 600°C (1.49 mmol g^{-1}), although still satisfactory when are compared with results obtained by previous authors [5, 11, 12, 25, 28–31]. Therefore, it could be said that in the case of the chemically activated hydrochars, it is true that as higher is the Vultra, higher is the CO_2 capture capacity [5]. More specifically, when comparing these produced adsorbents with other activated carbon of hydrothermally carbonized biomass, studied previously by other authors [8, 12, 25, 29], it can be observed that both the CO_2 uptake and V_{ultra} are in a similar range of values and even a bit better that these others.

3.2.Temperature-dependent adsorption of CO_2

Fig 4. shows the CO_2 isotherms at 25 and 75 °C for the physically activated sample at 850 °C during 3 h (i.e., AC_HTC_CO2_850_3) and the chemically activated hydrochars at 700°C (AC_HTC_KOH_2_700) and at 600°C (AC_HTC_KOH_5_600). Additionally, one of the N-doped samples (AC_HTC_ZN_700_CO2_3) was selected with the aim to compare, in more detail, its CO_2 capture capacity with both the physical and chemical activated carbons and determine the role of N-doping for CO_2 adsorption. At 25 °C, the highest CO_2 adsorption capacity at 15 kPa was 1.19 mmol g^{-1} for the AC_HTC_CO2_850_3 sample, which is in the lower range of those reported by previous authors at similar conditions of pressure and temperature (see Table 2) For adsorption at 75ºC, this physically activated sample is also the best material in terms of CO_2 uptake with a value of 0.55 mmol g^{-1}. Adsorption capacities up to 0.5 mmol g^{-1} have been previously reported by several authors at these conditions but not for physically activated carbons. Only Manyà et al. [5] reported a value of 0.465 mmol g^{-1} for a carbon physically activated with CO_2 at 800ºC. In this last work, the best behaviour showed by the physically activated carbon was attributed to the higher mesopore volumes that this sample possess when comparing with the chemically activated carbons, which can enhance the diffusion into micropores and ultra-micropores by shortening diffusion paths. However, the results obtained in this work show a lower mesopore volume for the AC_HTC_CO2_850_3

sample than for the chemically activated carbons and the N-doped samples also studied here. Therefore, in this case, the mesopores volume is not the responsible of the highest adsorption shown by this sample at these conditions.

Regarding the two chemically activated samples, the CO_2 uptake obtained for the AC_HTC_KOH_5_600 sample at 25ºC is only a bit lower (1.15 mmol g^{-1}) than the measured for the physically activated one analysed above. Nonetheless, the other chemically activated carbon studied, the AC_HTC_KOH_2_700, exhibited a value of CO_2 uptake below 1 (0.88 mmol g^{-1}) very far from the data obtained by other authors for chemically activated samples with KOH from different precursors [4, 6, 7, 24, 25, 29, 32–37]. Regarding the adsorption capacities at 75ºC, few data are available in bibliography for similar materials at that temperature. At similar conditions, the highest value of CO_2 uptake was found by Hao et al. [28] who reported a value of 0.5 mmol g^{-1} for a chemically activated carbon (with KOH at a mass ratio KOH/precursor of 2 and at 700ºC) from hydrothermally activated carbon. More recently, Manyà et al. [5] reported values within the range 032-0.39 mmol g^{-1} for several chemically activated carbons. Within this range is the value measured for the AC_HTC_KOH_5_600 sample (0.35 mmol g^{-1}) while the AC_HTC_KOH_2_700 sample exhibited a value of 0.25 mmol g^{-1}, far from the uptakes reported by these previous works.

Finally, the N-doped sample studied in this section showed a CO_2 capture capacity of 0.55 mmol g^{-1}, much lower than the obtained for the previous samples and very far from the values reported for N-doped porous carbons by recent works and summarized by Rouzitalab et al. [31] in their paper. Even worse is its performance at 75ºC with an adsorption capacity of just 0.12 mmol g^{-1}. This confirms, one more time, the negative role of the nitrogen in these adsorbents, which despite their high volume of ultra-micropores, they do not present high CO_2 capture capacities.

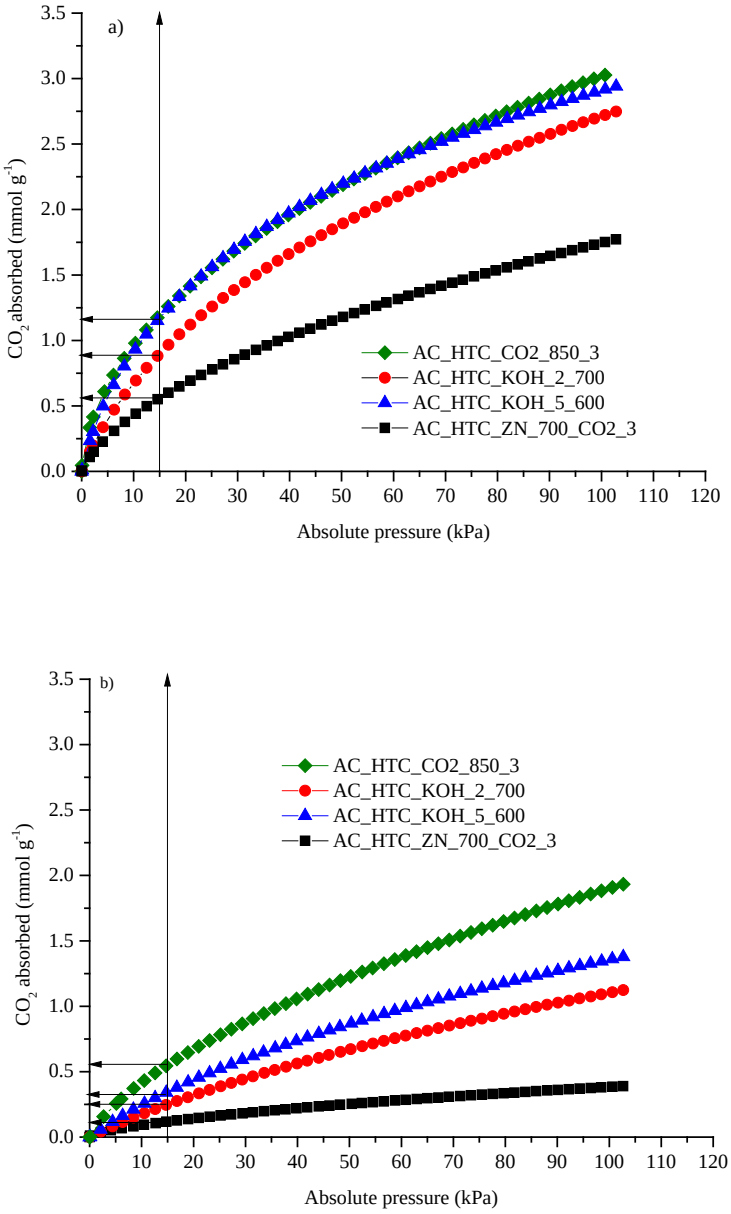

Fig 4. CO_2 adsorption isotherms at 25 °C (figure a) and 75 °C (figure b) for the selected samples: AC_HTC_CO2_850_3, AC_HTC_KOH_2_700, AC_HTC_KOH_5_600 and AC_HTC_ZN_700_CO2_3.

3.3.Apparent selectivity towards CO_2

From the experiments carried out in the TGA described in the experimental section, information related to the apparent adsorption rate and kinetic selectivity was obtained. These experiments were developed following the same procedure that Manyà et al.[5] described in

their work, being therefore the apparent CO_2-over-N_2 selectivity similarly calculated following the equation:

$$S = \left(\frac{x_{CO_2}}{x_{N_2}} \right) \sigma \quad (1)$$

where x_{CO_2} and x_{N_2} are the uptake capacities (in mmol g^{-1}) at 101.3 kPa after 1 min of CO_2 and N_2, respectively and σ represents the ratio of the CO_2 uptake at 15 kPa to that at 101.3 kPa from the corresponding adsorption isotherm. However, most of the values of selectivity found in the literature for others adsorbents (see Table 2) were predicted for CO_2-N_2 binary mixtures according to the ideal adsorption solution theory (IAST). Therefore, a comparison between the values obtained in this work from the single adsorption isotherms and these others would not be appropriate, given that as González et al. [6] and more recently, Manyà et al. [5] highlighted in their works, the N_2 adsorbed from a gas mixture could be up to half the quantity adsorbed in a single-component adsorption.

Table 2. Some CO_2 uptakes at 25 °C and 15 kPa and CO_2/N_2 selectivities reported in literature for activated porous carbons derived from different precursors.

Precursor (activation method)	Highest CO_2 uptake reported ($mmol.g^{-1}$)	Selectivity nCO_2/nN_2 *	Ref.
Rice husk char (chemical activation with KOH)	1.51	19.9	[4]
Vine shoot-derived biochar (physical activation with CO_2)	1.35	42.3	[5]
Almond shells (single-step activation with CO_2)	1.08	33	[6]
Coconut shell (chemical activation with KOH)	1.4	8.5	[7]
HTC from grass cuttings (physical activation with CO_2)	1.1	14.5	[8]
Camphor tree leaves (chemical activation with KOH)	1.1	27.5	[11]
Coconut shells (chemical activation with KOH)	1.4	19	[24]
HTC chars from empty fruit brunch (chemical activation with KOH)	1.2	11.2	[25]
Dried rice husk samples (chemical activation with KOH)	1.9	115	[27]
Eucalyptus Lignin (chemical activation with KOH)	1.8 (at 0ºC)	15	[28]

Precursor (activation method)	Highest CO_2 uptake reported ($mmol.g^{-1}$)	Selectivity nCO_2/nN_2 *	Ref.
HTC chars from Jujun grass (chemical activation with KOH)	1.5	Not available	[29]
Chemically synthetized polyindole Nanospheres (chemical activation with KOH)	1.6	81	[33]
Pyrolyzed coconut shells (chemical activation with KOH)	1.45	22	[34]
Melamine-doped phenolic-resins (chemical activation with KOH)	1.31	27.5	[35]
Pyrolized 1,3-bis (cynomethyl imidazolium) chloride (chemical activation with KOH)	1.70	62	[36]
Pyrolyzed pine nut shells (single-step activation with KOH)	2	8.4	[37]
Pomegranate peles (chemical activation with KOH)	1.25	15.1	[38]

*These values are apparent selectivities calculated similarly to the showed in this work or predicted for CO_2-N_2 binary mixtures according to the IAST model.

Table 3 summarizes the values obtained for the apparent CO_2-over-N_2 selectivities at 25 ºC and an adsorption time of 1min for all the samples studied. The corresponding dynamic adsorption curves at that temperature are showed in the Supplementary Data. Comparing the values obtained for the different adsorbents, there are three samples which stand out for their extraordinary high value: AC_HTC_CO2_700_1, AC_HTC_KOH_5_600 and AC_HTC_ZN_700_N2 being especially remarkable, the apparent selectivities of the first two, both over 300 for the dynamic adsorption at 101.3 kPa and 25ºC. No similar values have been found in the literature for any adsorbent (see Table 2) but it must be reminded that these are only estimates of selectivity, as the ideal would be to measure the values in dynamic conditions, as for example through adsorption/desorption cycles in a fixed bed column. Among the works [5, 6, 32] which reported values of CO_2-over-N_2 selectivities measured in similar conditions to this work (dynamic adsorption in fix bed adsorption unit) the value of 212 for the sample R6_2T, obtained by Liu et al. [27] is the closest one to the results obtained in this study but still far of the values of 331.9 and 315 found for the samples AC_HTC_CO2_700_1 and AC_HTC_KOH_5_600, respectively. It must be highlighted that although these two samples

present the highest selectivities among all the carbons studied in this work, they are not the best adsorbents in terms of CO_2 uptake, as it would be expected. In any case, these selectivities should be determined in dynamic conditions to get more accurate values.

Table 3. Apparent CO_2-over-N_2 selectivities and CO_2 uptakes at 25°C and an absolute pressure of 101.3 kPa deduced from the TGA adsorption tests.

Sample	CO_2 uptake after 1 min (mmol g^{-1})	Percentage of CO_2 adsorbed (%)[d]	Apparent selectivity (molar basis)
AC_HTC_CO2_700_1	0,79	51,2	331,9
AC_HTC_CO2_700_3	0,46	34,2	67,1
AC_HTC_CO2_850_1	0,84	73,2	56,5
AC_HTC_CO2_850_3	0,41	57,8	24,2
AC_HTC_KOH_2_600	0,17	29,8	13,0
AC_HTC_KOH_2_700	0,59	37,7	25,7
AC_HTC_KOH_5_600	1,09	62,3	315,0
AC_HTC_KOH_5_700	0,12	4,8	44,6
AC_HTC_ZN_700_N2	0,71	55,9	131,3
AC_HTC_ZN_700_CO2_1	0,38	49,2	49,0
AC_HTC_ZN_700_CO2_3	0,86	50,2	25,5

[d] Ratio [(uptake of CO_2 after 1 min)/ (uptake of CO_2 after 10 min)] in %

Comparing the results of the TGA experiments developed for all the HTC studied in this work at 25 ºC (Supplementary Data), it could be observed that as it was already reported by Manyà et al. [5] in their work, the physically activated carbons present higher CO_2 adsorption rates, not only than the chemically activated but also than the N-doped sorbents. This fact could be justified by the hierarchical pore structure showed by the physically activated samples which lead to higher diffusion rates, as Manyà et al. [5] pointed out in their work. In the case of the N-doped samples, it has been already indicated that despite their high V_{ultra} and V_{meso}, their affinity for CO_2 is very low and hence, their lower CO_2 uptakes.

3.4.Heat of adsorption

One of the critical factors to understand and design any adsorption process is the heat of adsorption, which as previous authors have reported [39], it measures the interaction

between the adsorbate molecules and the surface of the adsorbent. The common way to estimate the isosteric heat of adsorption is through the Clausius- Clapeyron equation (eq. 2). In this work, the values of Q_{st} were estimated by applying this equation to the CO_2 adsorption isotherms obtained at 0, 25 and 75ºC:

$$\frac{-Q_{st}}{R} = \left(\frac{\partial \ln p}{\partial T^{-1}} \right)_q \quad (2)$$

where q is a specific surface loading (mol kg^{-1}). The isosteric heat was obtained following the calculations explained previously by Manyà et al.[5] in their work. Figure 5 shows the isosteric heat of adsorption of the physically activated sample AC_HTC_CO2_850_3, the chemically activated samples AC_HTC_KOH_2_700 and AC_HTC_KOH_5_600 and the N-doped sample AC_HTC_CO2_700_3. The values obtained for the first two samples are similar to those reported by previous works [1, 5, 7-9, 11, 13, 16, 24, 28, 32, 34] while the other chemically activated adsorbent and the N-doped one, present much lower values, being specially low the Q_{st} calculated for the last one, which is below 4 kJ mol^{-1}. No similar values have been previously reported for other carbons and in fact, there is no clear relationship between N and the initial Q_{st} given that according to some authors [16, 40], it should be expected that the values of Q_{st} for the N-doped samples were superior than those shown by the other carbons demonstrating that the N functional groups play an important role in the initial interaction between CO_2 and the carbon surface. But on the other hand, the results obtained by Adeniran et al. [13] suggest that the presence of nitrogen does not have any effect on the Q_{st}. Regarding the variation in Q_{st} with the amount adsorbed, in Fig. 5 it could be observed a soft decrease in the Q_{st} with the CO_2 uptake for the studied samples, except the N-doped one, which isosteric heat slightly increases with the CO_2 absorbed. For the first, the decrease in Q_{st} with the increase of the CO_2 absorbed is related with the heterogeneity of the carbon [5, 16, 24, 32] being the N-doped sample more homogeneous as its isosteric heat remains almost constant.

Moreover, from the results obtained, it could be observed that as low is the CO_2 absorbed by the carbons, lower is low heat of adsorption presented.

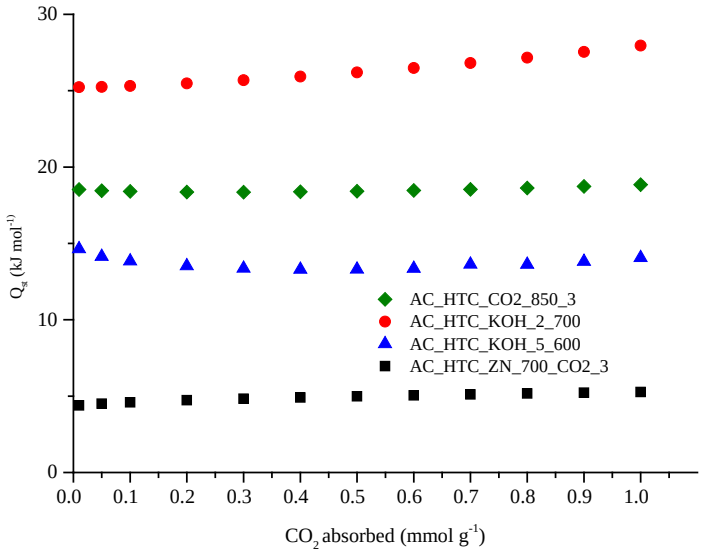

Fig 5. Isosteric heat of CO_2 adsorption as a function of the amount absorbed.

4. Conclusions

Hydrochars using olive mill waste as precursor have been prepared via three different methods: physical activation with CO_2, chemical activation using KOH and through a one-step hydrothermal carbonization to obtain N-doped adsorbents. In this way, carbons with closely matched porosity but either N-free or N-doped have been compared in terms of CO_2 uptake to clarify the effect of N-doping and pore size distribution. Concretely, when compared the adsorption capacity at 25 ºC and at an absolute pressure of 15 kPa, the physically activated sample AC_HTC_CO2_850_3 and the chemically activated AC_HTC_KOH_5_600 present similar behaviours. Nevertheless, when its performance in experimental conditions closer to postcombustion, that is, at higher temperature (75 ºC) is analysed, it seems that the physical activated carbon is the most promising option among all the samples studied. However, it would be also necessary to develop TGA experiments at this last temperature to get information about the apparent adsorption and kinetic selectivity which would allow to support this

affirmation. Regarding the N-doped samples prepared, the results obtained confirm the negative role of the nitrogen in these adsorbents, which despite their high volume of ultramicropores, they presented CO_2 capture capacities much lower than the N-free carbons studied in this work. In this sense, there is not an agreement between researchers and further investigations would be necessary to elucidate the role of N doping on CO_2 adsorption of these porous carbons.

Acknowledgements

This research received funding from the Spanish Ministry of Science, Innovation and Universities (ERANET-MED Project MEDWASTE, ref. PCIN-2017-048). The authors also acknowledge the funding from the Aragón Government (Ref. T22_17R), co-funded by FEDER 2014-2020 "Construyendo Europa desde Aragón".

References

[1] M. Yang, L. Guo, G. Hu, X. Hu, J. Chen, S. Shen, W. Dai, M. Fan, Adsorption of CO_2 by Petroleum Coke Nitrogen-Doped Porous Carbons Synthesized by Combining Ammoxidation with KOH Activation, Ind. Eng. Chem. Res. 55 (2016). https://doi.org/10.1021/acs.iecr.5b04038

[2] P. Gao, Y. Zhou, F. Meng, Y. Zhang, Z. Liu, W. Zhang, G. Xue, Preparation and characterization of hydrochar from waste eucalyptus bark by hydrothermal carbonization, Energy 97 (2016) 238–245. https://doi.org/10.1016/j.energy.2015.12.123

[3] J. Fang, L. Zhan, Y. Sik Ok, B. Gao, Minireview of potential applications of hydrochar derived from hydrothermal carbonization of biomass, J. Ind. Eng. Chem. 57 (2018) 15–21. https://doi.org/10.1016/j.jiec.2017.08.026

[4] D. Li, T. Ma, R. Zhang, Y. Tian, Y. Qiao, Preparation of porous carbons with high low-pressure CO_2 uptake by KOH activation of rice husk char, Fuel 139 (2015) 68–70. https://doi.org/10.1016/j.fuel.2014.08.027

[5] J.J. Manyà, B. González, M. Azuara, G. Arner, Ultra-microporous adsorbents prepared from vine shoots-derived biochar with high CO_2 uptake and CO_2/N_2 selectivity, Chem. Eng. J. 345 (2018) 631-639. https://doi.org/10.1016/j.cej.2018.01.092

[6] A.S. González, M.G. Plaza, F. Rubiera, C. Pevida, Sustainable biomass-based carbon adsorbents for post-combustion CO_2 capture, Chem. Eng. J. 230 (2013) 456–465. https://doi.org/10.1016/j.cej.2013.06.118

[7] L. Guo, J. Yang, G. Hu, X. Hu, L. Wang, Y. Dong, H. Dacosta, M. Fan, Role of Hydrogen Peroxide Preoxidizing on CO_2 Adsorption of Nitrogen-Doped Carbons Produced from Coconut Shell, ACS Sustainable Chem. Eng. 4 (2016) 2806−2813. https://doi.org/10.1021/acssuschemeng.6b00327

[8] W. Hao, E. Björkman, M. Lilliestråle, N. Hedin, Activated carbons prepared from hydrothermally carbonized waste biomass used as adsorbents for CO_2, Appl. Energy 112 (2013) 526–532. https://doi.org/10.1016/j.apenergy.2013.02.028

[9] L. Yue, Q. Xia, L. Wang, L. Wang, H. DaCosta, J. Yang, X. Hu, CO_2 adsorption at nitrogen-doped carbons prepared by K_2CO_3 activation of urea-modified coconut shell, J. Colloid Interface Sci. 511 (2018) 259–267. https://doi.org/10.1016/j.jcis.2017.09.040

[10] W. Xing, C. Liu, Z. Zhou, L. Zhang, J. Zhou, S. Zhuo, Z. Yan, H. Gao, G. Wang, S.Z. Qiao, Superior CO_2 uptake of N-doped activated carbon through hydrogen-bonding interaction, Energy Environ. Sci. 5 (2012) 7323–7327. https://doi.org/10.1039/c2ee21653a.

[11] J. Xu, J. Shi, H. Cui, N. Yan, Y. Liu, Preparation of nitrogen doped carbon from tree leaves as efficient CO_2 adsorbent, Chem. Phys. Lett. 711 (2018) 107–112. https://doi.org/10.1016/j.cplett.2018.09.038

[12] M. Sevilla, J.B. Parra, A.B. Fuertes, Assessment of the Role of Micropore Size and N - Doping in CO_2 Capture by Porous Carbons, ACS Appl. Mater. Interfaces 5 (2013) 6360−6368. https://doi.org/10.1021/am401423b

[13] B. Adeniran, R. Mokaya, Is N-Doping in Porous Carbons Beneficial for CO_2 Storage? Experimental Demonstration of the Relative Effects of Pore Size and N-Doping, Chem. Mater. 28 (2016) 994–1001. https://doi.org/10.1021/acs.chemmater.5b05020

[14] K.V. Kumar, K. Preuss, L. Lu, Z.X. Guo, M.M. Titirici, Effect of Nitrogen Doping on the CO_2 Adsorption Behavior in Nanoporous Carbon Structures: A Molecular Simulation Study, J. Phys. Chem. C. 119 (2015) 22310–22321. https://doi.org/10.1021/acs.jpcc.5b06017.

[15] J. Xu, J. Shi, H. Cui, N. Yan, Y. Liu, Preparation of nitrogen doped carbon from tree leaves as efficient CO_2 adsorbent, Chem. Phys. Lett. 711 (2018) 107–112. https://doi.org/10.1016/j.cplett.2018.09.038.

[16] J. Han, L. Zhang, B. Zhao, L. Qin, Y. Wang, F. Xing, The N-doped activated carbon derived from sugarcane bagasse for CO_2 adsorption, Industrial Crops & Products 128 (2019) 290–297. https://doi.org/10.1016/j.indcrop.2018.11.028.

[17] J.M. Ochando-pulido, S. Pimentel-moral, V. Verardo, A. Martinez-ferez, A focus on advanced physico-chemical processes for olive mill wastewater treatment, Separation and Purification Technology 179 (2017) 161–174. https://doi.org/10.1016/j.seppur.2017.02.004.

[18] A.K.Md. Muktadirul Bari Chowdhury, C.S. Akratos, D. V. Vayenas, S. Pavlou, Olive mill waste composting : A review, International Biodeterioration & Biodegradation 85 (2013) 108–119. https://doi.org/10.1016/j.ibiod.2013.06.019.

[19] J.A. Alburquerque, J. Gonzálvez, D. García, J. Cegarra, Agrochemical characterisation of "alperujo", a solid by-product of the two-phase centrifugation method for olive oil extraction, Bioresour.Technol. 1 (2004) 195–200. https://doi.org/10.1016/S0960-8524(03)00177-9.

[20] M. Azuara, B. Baguer, J.I. Villacampa, N. Hedin, J.J. Manyà, Influence of pressure and temperature on key physicochemical properties of corn stover-derived biochar, Fuel 186 (2016) 525–533. https://doi.org/10.1016/j.fuel.2016.08.088.

[21] M. Azuara, E. Sáiz, J.A. Manso, F.J. García-Ramos, J.J. Manyà, Study on the effects of using a carbon dioxide atmosphere on the properties of vine shoots-derived biochar, J. Anal. Appl. Pyrolysis. 124 (2017) 719–725. https://doi.org/10.1016/j.jaap.2016.11.022.

[22] K. C. Kim, T. Yoon, Y. Bae, Applicability of using CO_2 adsorption isotherms to determine BET surface areas of microporous materials, Microporous Mesoporous Mater. 224 (2016) 294–301. https://doi.org/10.1016/j.micromeso.2016.01.003.

[23] S. Shahkarami, A.K. Dalai, J. Soltan, Y. Hu, D. Wang, Selective CO_2 Capture by Activated Carbons : Evaluation of the Effects of Precursors and Pyrolysis Process, Energy Fuels 29 (2015) 7433−7440. https://doi.org/10.1021/acs.energyfuels.5b00470.

[24] J. Chen, J. Yang, G. Hu, X. Hu, Z. Li, S. Shen, M. Radosz, M. Fan, Enhanced CO_2 Capture Capacity of Nitrogen-Doped Biomass-Derived Porous Carbons, ACS Sustainable Chem. Eng. 4 (2016) 1439−1445. https://doi.org/10.1021/acssuschemeng.5b01425.

[25] G.K. Parshetti, S. Chowdhury, R. Balasubramanian, Biomass derived low-cost microporous adsorbents for efficient CO_2 capture, Fuel. 148 (2015) 246–254. https://doi.org/10.1016/j.fuel.2015.01.032.

[26] L. Wang, L. Rao, B. Xia, L. Wang, L. Yue, Y. Liang, H. DaCosta, X. Hu, Highly efficient CO_2 adsorption by nitrogen-doped porous carbons synthesized with low-temperature sodium amide activation, Carbon N. Y. 130 (2018) 31–40. https://doi.org/10.1016/j.carbon.2018.01.003.

[27] X. Liu, C. Sun, H. Liu, W.H. Tan, W. Wang, C. Snape, Developing hierarchically ultra-micro/mesoporous biocarbons for highly selective carbon dioxide adsorption, Chem. Eng. J. 361 (2019) 199–208. https://doi.org/10.1016/j.cej.2018.11.062.

[28] W. Hao, F. Björnerbäck, Y. Trushkina, M.O. Bengoechea, G. Salazar-Alvarez, T. Barth, N. Hedin, High-performance Magnetic Activated Carbon from Solid Waste from Lignin Conversion Processes. Part I: Their Use as Adsorbents for CO_2, Energy Procedia 114 (2017) 6272–6296. https://doi.org/10.1021/acssuschemeng.6b02795.

[29] H.M. Coromina, D.A. Walsh, R. Mokaya, Biomass-derived activated carbon with simultaneously enhanced CO_2 uptake for both pre and post combustion capture applications, J. Mater. Chem. A. 4 (2016) 280–289. https://doi.org/10.1039/c5ta09202g.

[30] M. Sevilla, A.S.M. Al-Jumialy, A.B. Fuertes, R. Mokaya, Optimization of the Pore Structure of Biomass-Based Carbons in Relation to Their Use for CO_2 Capture under Low and High-Pressure Regimes, ACS Appl. Mater. Interfaces 10 (2018) 1623−1633 https://doi.org/10.1021/acsami.7b10433.

[31] Z. Rouzitalab, D. M. Maklavany, A. Rashidi, S. Jafarinejad, Synthesis of N-doped nanoporous carbon from walnut shell for enhancing CO_2 adsorption capacity and separation, J. Environ. Chem. Eng. 6 (2018) 6653–6663. https://doi.org/10.1016/j.jece.2018.10.035.

[32] X. Ren, H. Li, J. Chen, L. Wei, A. Modak, H. Yang, Q. Yang, N-doped porous carbons with exceptionally high CO_2 selectivity for CO_2 capture, Carbon 114 (2017) 473–481. https://doi.org/10.1016/j.carbon.2016.12.056.

[33] J. Yang, L. Yue, X. Hu, L. Wang, Y. Zhao, Y. Lin, Y. Sun, H. Dacosta, L. Guo, Efficient CO_2 Capture by Porous Carbons Derived from Coconut Shell, Energy Fuels 31 (2017) 4287−4293. https://doi.org/10.1021/acs.energyfuels.7b00633.

[34] H. Cong, M. Zhang, Y. Chen, K. Chen, Y. Hao, Y. Zhao, L. Feng, Highly selective CO_2 capture by nitrogen enriched porous carbons, Carbon 92 (2015) 297–304. https://doi.org/10.1016/j.carbon.2015.04.052.

[35] G. Sethia, A. Sayari, Comprehensive study of ultra-microporous nitrogen-doped activated carbon for CO_2 capture, Carbon 93 (2015) 68–80. https://doi.org/10.1016/j.carbon.2015.05.017.

[36] S. Deng, H. Wei, T. Chen, B. Wang, J. Huang, G. Yu, Superior CO_2 adsorption on pine nut shell-derived activated carbons and the effective micropores at different temperatures, Chem. Eng. J. 253 (2014) 46–54.

https://doi.org/10.1016/j.cej.2014.04.115.

[37] J. Serafin, U. Narkiewicz, A.W. Morawski, R.J. Wróbel, B. Michalkiewicz, Highly microporous activated carbons from biomass for CO_2 capture and effective micropores at different conditions, Journal of CO_2 Utilization 18 (2017) 73–79. https://doi.org/10.1016/j.jcou.2017.01.006.

[38] E. Jang, S.W. Choi, S-M. Hong, S. Shin, K.B. Lee, Development of a cost-effective CO_2 adsorbent from petroleum coke via KOH activation, Appl. Surf. Sci. 429 (2017) 62–71. https://doi.org/10.1016/j.apsusc.2017.08.075.

[39] M.S. Shafeeyan, W.M.A.W. Daud, A. Shamiri, N. Aghamohammadi, Adsorption equilibrium of carbon dioxide on ammonia-modified activated carbon, Chem. Eng. Res. Des. 104 (2015) 42–52. https://doi.org/10.1016/j.cherd.2015.07.018.

[40] Y. Xia, R. Mokaya, G.S. Walker, Y. Zhu, Superior CO_2 adsorption capacity on N-doped, high-surface-area, microporous carbons templated from zeolite, Adv. Energy Mater. 1 (2011) 678–683. https://doi.org/aenm.201100061.